

# Thermohydrodynamic analysis of concentric journal bearing with heterogeneous slip/no-slip pattern

*by* Paryanto Paryanto

---

**Submission date:** 15-Mar-2025 07:23AM (UTC+0700)

**Submission ID:** 2415009583

**File name:** Thermohydrodynamic\_Analysis\_of\_Concentric.pdf (577.52K)

**Word count:** 2724

**Character count:** 14359

# Thermohydrodynamic Analysis of Concentric Journal Bearing with Heterogeneous Slip/No-Slip Pattern

Mohammad Tauviquirrahman<sup>1, a)</sup>, Michael Wijaya<sup>1, b)</sup>, M. Fadhli Afif<sup>1, c)</sup>, P. Paryanto<sup>1, 2, d)</sup>

<sup>1</sup>Laboratory for Engineering Design and Tribology, Department of Mechanical Engineering, Faculty of Engineering, Diponegoro University, Jl. Prof. Soedarto, Tembalang, Semarang 50275, Indonesia

<sup>2</sup>Institute for Factory Automation and Production Systems (FAPS), Friedrich Alexander Universität Erlangen Nürnberg J.Egerlandstr. 7–9, 91058 Erlangen, Germany

<sup>a)</sup> mohammad.tauviquirrahman@ft.undip.ac.id

<sup>b)</sup> Corresponding author: michaelwijayacenter@gmail.com, mohammad.tauviquirrahman@ft.undip.ac.id

<sup>c)</sup> fadhliafifm@gmail.com

<sup>d)</sup> paryanto@gmail.com

**Abstract.** The performance of hydrodynamic journal bearing is heavily influenced by the slip boundary. The slip boundary can be induced by the hydrophobic coating. The favorable influence of slip on thermal behavior, on the other hand, has received less attention. Parameters related to thermo-hydrodynamic properties of heterogeneous slip/no slip bearing under concentric condition are investigated in this study using computational fluid dynamics (CFD). When operating at various shaft rotational speeds, the thermo hydrodynamic behavior of heterogeneous slip/no-slip bearings is explored in terms of lubrication pressure, temperature, distribution, volume fraction of vapor, and load-carrying capabilities. The cavitation condition is depicted using the multiphase cavitation model. It is found that the tribological performance of journal bearings is substantially influenced by shaft speed. Besides, the maximum hydrodynamic lubricating pressure produced proportionally climbs as the shaft speed on the journal bearing increases. The findings show that as the shaft speed increases, so does the temperature of the lubricant. Moreover, it is found that the effect of slip is desirable in all simulated conditions since it enhances the load-carrying capacity of the bearing, just as shaft speed does.

## INTRODUCTION

Recently, a deterministic hydrophobic coating has been applied to the bearings on purpose. Engineered slip/no-slip patterns, in which slip occurs in some zones but not others, are gaining popularity as a way to improve load support and reduce bearing friction. Throughout most frictional coupling systems, emphasis has been placed on the application of a (super)hydrophobic coating to improve tribological performance and extend bearing lifespan. Early research suggested that due to its non-stick properties, such a covering could cause wall slip [1, 2].

It is worth mentioning early study [3] on the impact of partially textured slip sliders and journal bearings, on load-carrying capacity enhancement, and some reduction of friction coefficient. On the other hand, Kalavathi et al. [4] investigate the effect of slip parameters on a journal bearing that has a heterogeneous slip/no-slip zone, finding a substantial correlation between the velocity slip and lubrication performance. Furthermore, the study of Zhang et al. [5] contains a process for adjusting the boundary slip region on bearing sliders, which has been found to greatly improve the bearing's performance characteristics. Tauviquirrahman et al. [6] also conducted a related study in which a journal bearing with a 0.6 eccentricity is investigated with slip/no-slip zone variations, which concludes that the slip zone affects the tribological performance of a journal bearing. The work of Susilowati et al. [7] then looks into a textured surface bearing with a slip zone using a modified Reynolds equation. It was found that combining texturing and slip approaches had a substantial impact on improving a bearing's tribological performance. Bhattacharya et al.

[8], who studied the stability of rotors supported on fluid film journal bearings with multilocal slip and no-slip zones at the bush–film interface, comes to a similar conclusion. Similar to multilobe bearings, the trend of pressure with numerous slip/no-slip zones is similar. In addition, the slip zone geometry must be chosen with caution. Lin et al. [9] proved that a well-designed partial slip surface may increase tribological performance on a hybrid high-speed journal bearing.

Based on the literature survey, there has been very little research on the study of heterogeneous slip/no-slip journal bearings using multiphase flow analysis to model cavitation. Furthermore, no research was conducted on the bearing in the concentric condition. By that, greater efforts in the domain of heterogeneous slip/no-slip bearings are required to give a useful reference step for designing a multiphase thermo-hydrodynamic (THD) model was created in this study to get a more accurate prediction, taking into account lubricating phase transition. This multiphase analysis-based realistic cavitation treatment would allow for the prediction of the rupture lubricant and boundary reformations. Furthermore, by using a combined vapor transport and Navier–Stokes solution, this paper numerically investigates the heterogeneous slip/no-slip journal bearing in terms of thermal, and cavitation.

## MODELLING

In actuality, the surfaces' slip boundary can be designed by altering roughness [10] and wettability [11] qualities. The modified model of Navier slip, as stated in the Equation below, is used in the numerical framework. If the shear stress  $\tau$  of the fluid and solid bypass a certain value of criticality  $\tau_{cr}$ , the boundary of slip appears, according to this concept. The associated slip velocity is determined by:

$$\text{If } \tau < \tau_{cr}, u_s = 0 \quad (1)$$

$$\text{If } \tau \geq \tau_{cr}, u_s = (\tau - \tau_{cr}) \frac{b}{\mu}$$

The slip boundary is given at  $\tau_{cr}$ , which is the critical shear stress. There  $u_s$  is the velocity of slip, and  $b$  corresponds to the length of the slip.  $\mu$  is the viscosity of the lubricant at 40 °C. The slip length  $b$  indicates the amount of slip that occurs when the surface comes into contact with a given lubricant [12]. At a constant slip length  $b$ , Equation (1) states that the velocity of the slip phenomena increases accordingly with the rise of the shear stress. Based on Equation (2), a user-defined function is built in this study to represent the boundary in a foreordained way. The uniform slip length is used in all of the calculations. Based on published works [13], the slip coefficient is set to 0.05 m<sup>2</sup>/kg is employed.

A series of equations known as the Navier–Stokes equation explains the motion of a fluid. This equation indicates that the internal force implied by viscosity and the pressure acting from external viscous force towards the region of fluid determine the change in momentum of the fluid particles. As a result, based on the principle of conservation of momentum, the Navier – Stokes equation represents the equilibrium of forces operating on a Newtonian fluid in a viscous flow. The idea of conservation of momentum underpins the general equation for Newtonian fluid motion in viscous flow. The Navier–Stokes equation is constructed by describing the change in velocity of fluid particles and applying the basic relationship between fluids and the momentum equation.

$$\rho_f \frac{D\vec{V}}{Dt} = -\vec{\nabla}P + \rho_f \vec{g} + \mu_f \nabla^2 \vec{V} \quad (2)$$

The Navier– Stokes equation requires the concept of mass conservation to be solved. A continuity equation is required for this. This equation fits the theoretical requirements for solving the Navier– Stokes equation.

$$\frac{\partial \rho_f}{\partial t} + \nabla \cdot (\rho_f \vec{V}) = 0 \quad (3)$$

where  $\nabla$  is the operator vector,  $\rho_f$  indicates lubricating fluid density,  $\vec{V}$  indicates lubricating fluid velocity vector, and  $t$  shows time spent computing the lubricating fluid under unsteady flow conditions.

Cavitation is represented in this work as a model of mixture that depicts two phases liquid flow and vapor. The model of mixture solves the equation of mixture and authorizes velocity relatively to determine the scattered phases [14].

$$\nabla \cdot (\alpha_v \rho_v \vec{V}) = R_g - R_c \quad (4)$$

$\alpha_v$  stands for the volume fraction of vapor, and  $\rho_v$  stands for the density of the vapor. In cavitation, mass flow between both phases is accounted by  $R_g$  and  $R_c$ . The equation of Rayleigh Plesset gives an appropriate prediction of the

cavitation of the vapor phase, and is used to model them. In a liquid, a single bubble of vapors' growth is represented using this equation, which is governed by the following equation.

$$R_{bl} \frac{d^2 R_{bl}}{dt^2} + \frac{3}{2} \left( \frac{dR_{bl}}{dt} \right)^2 = \frac{p_{bl} - p}{\rho} - \frac{2\sigma}{\rho R_{bl}} - 4 \frac{\mu}{\rho R_{bl}} \frac{dR_{bl}}{dt} \quad (5)$$

Equation (5) is simplified by ignoring surface tension and the acceleration of bubble formation:

$$\frac{dR_{bl}}{dt} = \left( \frac{2}{3} \frac{p_{bl} - p}{\rho} \right)^{1/2} \quad (6)$$

In the cavitation model, Equation (4) provides a physical way to anticipate bubble dynamics' impacts. It may also be used to determine the spread of void [15]. The multiphase cavitation expression of Zwart-Gerber-Belamri is used since it requires less time [14]. The final form of cavitation for the model of Zwart-Gerber-Belamri is as follows,

$$p \leq p_{sat}, \quad R_g = F_{evap} \frac{3\alpha_{max}(1-\alpha_v)\rho_v}{R_{bl}} \sqrt{\frac{2}{3} \frac{p_{sat} - p}{\rho}} \quad (7)$$

$$p \geq p_{sat}, \quad R_c = F_{cond} \frac{3\alpha_v \rho_v}{R_{bl}} \sqrt{\frac{2}{3} \frac{p - p_{sat}}{\rho}} \quad (8)$$

where  $p_v$  saturation vapor pressure of liquid at a certain temperature,  $F_{evap}$  which is the coefficient of evaporation,  $F_{cond}$  refers to the coefficient of condensation.

## METHODOLOGY

Figure 1 shows a three-dimensional model schematic of the heterogeneous slip/no-slip journal bearing varying the rotational speed  $n$ , which clarifies the primary parameters and the computational domain shape. As illustrated in Figure 2, the slip/no-slip arrangement is applied on the fixed surface that represents the bearing sleeve. Based on previous research [16,17,18], the slip/no-slip arrangement carrying a rectangular shape is of special relevance in the current work. The slip is used in part on the convergent area for increased load support generation. The slip zone is constructed following the coordinate, as in the angle of circumference as shown by  $\theta$  with an angel of  $0^\circ$ , using the location reference which is scaled at  $h_{max}$ , until the  $\theta$  of  $180^\circ$ . The model of the simulations' parameters are listed in Table 1.

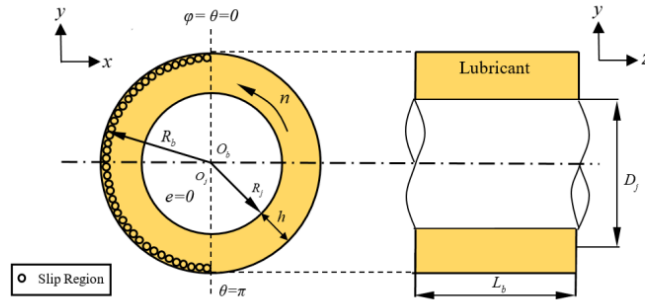
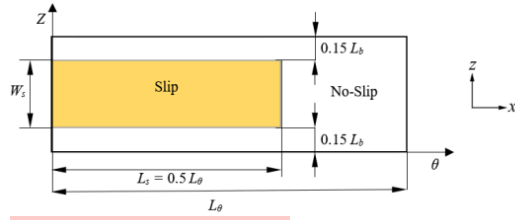


FIGURE 1 Heterogeneous slip/no-slip schematic of a journal bearing



**FIGURE 2** Heterogeneous slip/no-slip design for the bearing

**TABLE 1.** Parameters associated with the model.

Parameters	Value	Unit
Radius of Journal, $R_j$	40	mm
Bearing length $L_b$	80	mm
Radial clearance $c$	0.04	mm
Angular velocity $n$	100, 500, 1000, 3000, and 5000	rpm
Dynamic viscosity of oil $\mu$ (40°C)	0.0125	Pa.s
Density of oil $\rho$ (40°C)	850	kg/m <sup>3</sup>
Specific heat of oil $C_p$ (40°C)	1944	J/kg.K
Thermal conductivity of oil $\lambda$ (40°C)	0.12789	W/m.K
Dynamic viscosity of vapor $\mu_v$	$2 \times 10^{-5}$	Pa.s
Vapor density $\rho_v$	10.95	kg/m <sup>3</sup>
Vapor specific heat $C_{pv}$	2430	J/kg.K
Vapor thermal conductivity $\lambda_v$	0.0178	W/m.K
Vapor saturation pressure $p_v$	29,185	Pa

A three-dimensional mesh is used to discretize the spatial fluid domain in this paper. In this work, four layers of the grid is used. Furthermore, mesh dependence research is carried out for the given problem in order for determining the correctness of the results. As a result, several mesh sizes are used in computer simulations to assure independent mesh outputs. The element size in the current study is 0.5 mm, and the grid number employed for the calculations is roughly 250,000.

During the calculation in ANSYS FLUENT® software, in order to calculate the cavitation zone, the model of MIXTURE is used. The computational domain's boundary condition for CFD-based thermohydrodynamic analysis is configured as illustrated in Figure 3: the pressure of ambience (zero), is assumed as input and output borders. Oil goes into the bearing at a constant temperature 300 °K. The temperature in the outflow part is fixed to 318°K.

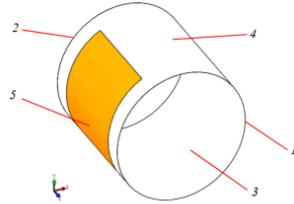
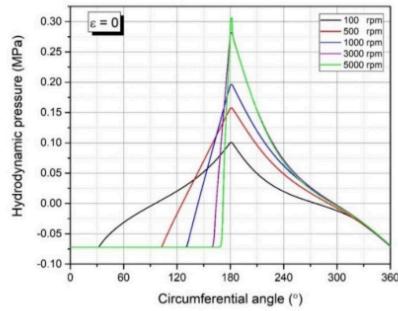


**FIGURE 3** Computational boundary conditions: (1) temperature inlet and pressure inlet (2) temperature and pressure outlet (3) rotary wall (4) static wall without slip (5) static wall with slip.

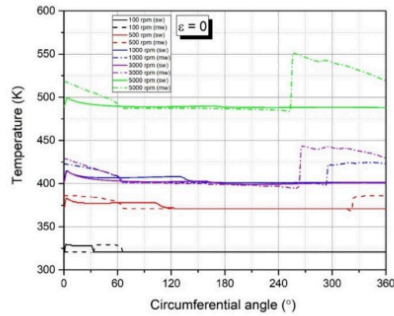
To obtain the results, SIMPLE velocity pressure coupling approach is used in this simulation. The discretization scheme of second-order upwind is chosen, while the QUICK technique is applied for the fraction of volume. Furthermore, the first-order upwind is also used for the discretization of turbulent kinetic energy, and the turbulent dissipation rate is done using the. The energy and pressure convergence precisions used in this investigation are  $1.0 \times 10^{-6}$  and  $1.0 \times 10^{-4}$ .

## RESULTS AND DISCUSSION

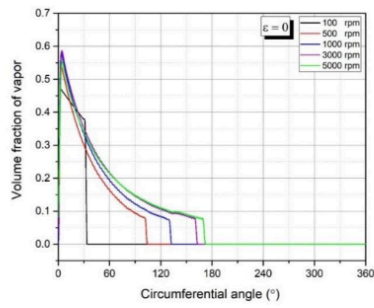
At various shaft speeds, starting at 100 RPM, 500 RPM, 1000 RPM, 3000 RPM, and up to 5000 RPM, the performance of heterogeneous slip/no-slip journal bearing under concentric conditions (i.e. zero eccentricity ratio) is investigated. It should be noted, in the real application, for concentric condition, the lubrication failure will occur in the conventional bearing due to the absence of the additional load support. The hydrodynamic distribution of pressure with slip included is depicted in Figure 5(a) which shows that as the shaft speed on the bearing rises, so does the hydrodynamic pressure of the lubricant produced. As illustrated in Figure 5, the maximum hydrodynamic pressure rises due to an increase in the volume fraction of the vapor created due to cavitation as reflected in Figure 5(c). In addition, as illustrated in Figure 5(b), an increase in shaft speed in the journal bearing induces an increase in the maximum temperature of the lubricant. It can also be observed that the temperature profile also reveals the difference in values between the stationary and moving walls indicating that the isothermal assumption which was often used in the previously published works was questionable.



(a)



(b)



(c)

**FIGURE 5** Distribution of (a) the pressure, (b) temperature, and (c) volume fraction of vapor along the contacting surface.

Figure 6 shows the comparison of the load-carrying capacity<sup>1</sup> between the conventional bearing and the heterogeneous slip/no-slip pattern. It is revealed that a heterogeneous slip/no-slip pattern produces the load-carrying capacity, while for conventional bearing, the zero load-carrying capacity is achieved. This is because, under concentric condition, no hydrodynamic pressure is generated due to the absence of the wedge effect. This is different when a heterogeneous slip/no-slip pattern is applied. The slip boundary leads to a reduced pressure gradient which creates the pressure jump to a higher values depicted in Figure 5(a).

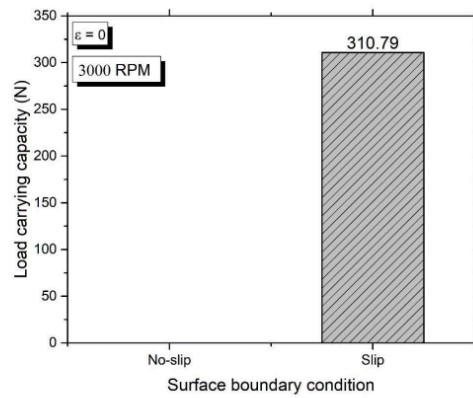


**FIGURE 6** Conventional vs heterogeneous slip/no-slip bearings in terms of load-carrying capacity

## CONCLUSION

The current study examines the THD behavior of heterogeneous slip/no-slip journal bearings, with key performance parameters such as the load-carrying capacity of the bearing, temperature, and hydrodynamic pressure. The impacts of shaft rotational speed are explored, as well as the possible benefits of using a heterogeneous slip/no-slip pattern. These conclusions can be drawn as follows: (1) the assumption of isothermal in heterogeneous slip/no-slip bearing cannot be valid considering the moving and stationary wall gives a different trend of temperature (2) under the concentric condition, the heterogeneous slip/no-slip pattern gives a beneficial effect on improving the performance while for the conventional bearing, the performance can fail.

## ACKNOWLEDGMENT

This research is fully funded by Universitas Diponegoro through RPI Grant, No. 233-29/UN7.6.1/PP/2022

## REFERENCES

1. M. Kalin and M. Polajnar, *Tribol. Lett.* **52**, 185-194 (2013)
2. C. Cottin-Bizonne, B. Cross, A. Steinberger, and E. Charlaix, *Phys. Rev. Lett.* **94**, 056102 (2005)
3. T. V. V. L. N. Rao, A. M. A. Rani, T. Nagarajan, and F. M. Hashim, *Tribol. Int.* **52**, 121 (2012)
4. G.K. Kalavathi, P.A. Dinesh, and K. Gururajan, *Tribol. Int.* **102**, 174 (2016)
5. H. Zhang, Y. Liu, S. Dai, F. Li, and G. Dong, *Tribol. Int.* **168**, 107446 (2022)
6. M. Tauviquirrahman, M. F. Afif, P. Paryanto, J. Jamari, and W. Caesarendra, *Fluids* **6**(2), 48 (2021)
7. S. Susilowati, M. Tauviquirrahman, J. Jamari, and A. P. Bayuseno, *Tribol. - Mater. Surf. Interfaces* **10**(2), 86-89 (2016)
8. A. Bhattacharya, J. K. Dutt, and R. K. Pandey, *ASME J. Tribol.* **139**, 6 (2017)
9. Q. Lin, Z. Wei, Y. Zhang, and N. Wang, *Proc. Inst. Mech. Eng. J: J. Eng. Tribol.* **230**, 9 (2016)
10. C. Neto, D. R. Evans, E. Bonaccorso, H. Butt, and V. S. J. Craig, *Rep. Prog. Phys.* **68**, 2859 (2005)
11. H. A. Spikes, *Proc. Inst. Mech. Eng. J: J. Eng. Tribol.* **217**, 1 (2003)
12. J. H. Choo, R. P. Glovnea, A. K. Forrest, and H. A. Spikes, *ASME J. Tribol.* **129**, 611 (2007)
13. M. Tauviquirrahman, W. K. Ajie, E. Yohana, M. Muchammad, J. Jamari, *Int. J. Eng. Technol.* **8**(2), 913-921 (2016)
14. ANSYS Fluent: User Manual, version 16.0; ANSYS Inc.: Canonsburg, PA, USA, (2017)
15. P. J. Zwart, A. G. Gerber, and T. Belamri, 2004 International Conference on Multiphase Flow (Yokohama, Japan, 2004), 152
16. M. Tauviquirrahman, R. Ismail, J. Jamari, D.J. Schipper, *Comput. Fluids* **79**, 27-43 (2013)
17. H. Zhang, M. Hua, G. Dong, D. Zhang, and K. Chin, *Tribol. Int.* **79**, 32 (2014)
18. S. Cui, C. Zhang, M. Fillon, and L. Gu, *Tribol. Int.* **145**, 106137 (2020)
19. Q. Li, S. Zhang, Y. Wang, W. Xu, and Z. Wang, *Ind. Lubr. Tribol.* **71**, 109 (2019)



# Thermohydrodynamic analysis of concentric journal bearing with heterogeneous slip/no-slip pattern

## ORIGINALITY REPORT

6%

SIMILARITY INDEX

6%

INTERNET SOURCES

%

PUBLICATIONS

0%

STUDENT PAPERS

## PRIMARY SOURCES

1

[www.mdpi.com](http://www.mdpi.com)

Internet Source

6%

Exclude quotes Off

Exclude bibliography On

Exclude matches Off